Targeted exon skipping of a *CEP290* mutation rescues Joubert syndrome phenotypes in vitro and in a murine model

Simon A. Ramsbottom[a,1], Elisa Molinari[a,1], Shalabh Srivastava[a,b,1], Flora Silberman[c], Charline Henry[c], Sumaya Alkanderi[a], Laura A. Devlin[a], Kathryn White[d], David H. Steel[a,e], Sophie Saunier[c], Colin G. Miles[a,2], and John A. Sayer[a,b,f,2]

[a]Institute of Genetic Medicine, Newcastle University, International Centre for Life, Central Parkway, Newcastle upon Tyne NE1 3BZ, United Kingdom; [b]Renal Services, The Newcastle Hospitals NHS Foundation Trust, Newcastle upon Tyne NE7 7DN, United Kingdom; [c]Laboratory of Hereditary Kidney Diseases, INSERM UMR 1163, Sorbonne Paris Cité University, Imagine Institute, 75015 Paris, France; [d]Electron Microscopy Research Services, Medical School, Newcastle University, Newcastle upon Tyne NE2 4HH, United Kingdom; [e]Sunderland Eye Infirmary, Sunderland SR2 9HP, United Kingdom; and [f]National Institute for Health Research Newcastle Biomedical Research Centre, Newcastle upon Tyne NE4 5PL, United Kingdom

Edited by Martin R. Pollak, Harvard Medical School, Beth Israel Deaconess Medical Center, Brookline, MA, and approved October 19, 2018 (received for review June 1, 2018)

Genetic treatments of renal ciliopathies leading to cystic kidney disease would provide a real advance in current therapies. Mutations in *CEP290* underlie a ciliopathy called Joubert syndrome (JBTS). Human disease phenotypes include cerebral, retinal, and renal disease, which typically progresses to end stage renal failure (ESRF) within the first two decades of life. While currently incurable, there is often a period of years between diagnosis and ESRF that provides a potential window for therapeutic intervention. By studying patient biopsies, patient-derived kidney cells, and a mouse model, we identify abnormal elongation of primary cilia as a key pathophysiological feature of *CEP290*-associated JBTS and show that antisense oligonucleotide (ASO)-induced splicing of the mutated exon (41, G1890*) restores protein expression in patient cells. We demonstrate that ASO-induced splicing leading to exon skipping is tolerated, resulting in correct localization of CEP290 protein to the ciliary transition zone, and restoration of normal cilia length in patient kidney cells. Using a gene trap *Cep290* mouse model of JBTS, we show that systemic ASO treatment can reduce the cystic burden of diseased kidneys in vivo. These findings indicate that ASO treatment may represent a promising therapeutic approach for kidney disease in *CEP290*-associated ciliopathy syndromes.

Joubert syndrome | Cep290 | cystic kidney | antisense oligonucleotide therapy | ciliopathy

Joubert syndrome (JBTS) is an archetypal ciliopathy syndrome, characterized by multisystem involvement, including retinal dystrophy and degeneration, cerebellar vermis aplasia, and nephronophthisis. JBTS is incurable and nephronophthisis represents the major cause of pediatric renal failure (1). Studying the molecular genetics of JBTS has led to the discovery of numerous genes underlying this disorder, which all encode protein products associated with the primary cilium. *CEP290* is the most common genetic cause of JBTS with a cerebello-retinal-renal phenotype (2). Mutations in *CEP290* may give rise to additional phenotypes as part of a disease spectrum including Leber congenital amaurosis (LCA), Senior Loken syndrome, Meckel Gruber syndrome, and Bardet Biedl syndrome (3–6). The *CEP290* gene has 54 exons that encode a protein located at the transition zone of the primary cilium where it is thought to play a gatekeeper role in the entry and exit of proteins from the ciliary axoneme (7). Ciliary signaling mechanisms such as the Sonic hedgehog (SHH) pathway have been shown to be disrupted in both mouse models of JBTS and primary patient renal epithelial cells; pharmacological manipulation of SHH signaling has been shown to ameliorate features of the disease, such as primary cilia defects (8, 9). However, such pharmacological interventions do not correct the primary lesion and, particularly in the case of modulation of SHH signaling, carry a risk of unwanted side effects.

Recent studies have suggested alternative therapeutic strategies for ciliopathies that directly correct the genetic lesion, in particular targeting *CEP290* mutations in LCA (10). The most common cause of LCA is an intronic mutation that creates a splice donor site and a pseudoexon, disrupting the CEP290 transcript (11). Treatment with a splice-blocking antisense oligonucleotide (ASO) was able to restore the normal transcript in both patient cell lines and a mouse model of LCA (10). The majority of *CEP290* mutations causing JBTS are within the coding sequence, which is more suited to gene replacement therapy. However, the size of the gene (54 exons) and its protein product (290 kDa) pose a considerable challenge for conventional, viral-based, gene replacement therapies, although lentiviral vector delivery of full-length *CEP290* has been used successfully in patient fibroblast cells (12). Following a report of a patient with a mild LCA phenotype associated with nonsense-mediated alternative splicing of *CEP290* (11), an extensive study of endogenous (wild-type) splicing revealed widespread, low-level alternative splicing that

Significance

The treatment of genetic kidney disease is challenging, as this requires both the correction of the underlying gene defect and the delivery of the treatment. Here we show that by using antisense oligonucleotides, we can induce exon skipping of a mutated exon in *CEP290*, within renal epithelial cells derived from a patient with a ciliopathy syndrome called Joubert syndrome. This treatment rescues the truncated CEP290 protein to a near full-length protein and restores the ciliary phenotype. In a *Cep290* murine model of Joubert syndrome, exon skipping is achievable with systemic treatment of an antisense oligonucleotide, which rescues both the ciliary and kidney disease phenotypes. This work paves the way toward personalized genetic therapies in patients with inherited kidney diseases.

Author contributions: S.A.R., E.M., C.G.M., and J.A.S. designed research; S.A.R., E.M., S. Srivastava, F.S., C.H., S.A., L.A.D., K.W., D.H.S., S. Saunier, C.G.M., and J.A.S. performed research; S.A.R., E.M., S. Srivastava, S.A., D.H.S., S. Saunier, and C.G.M. analyzed data; and S.A.R., E.M., C.G.M., and J.A.S. wrote the paper.

The authors declare no conflict of interest.

This article is a PNAS Direct Submission.

[1]S.A.R., E.M., and S. Srivastava contributed equally to this work.

[2]To whom correspondence may be addressed. Email: colin.miles@newcastle.ac.uk or john.sayer@newcastle.ac.uk.

This article contains supporting information online at www.pnas.org/lookup/suppl/doi:10.1073/pnas.1809432115/-/DCSupplemental.

Published online November 16, 2018.

could be modeled to predict genetic pleiotropy associated with *CEP290* mutations (13). Indeed, confirming this hypothesis, endogenous basal exon skipping and nonsense-associated altered splicing has been documented in patient fibroblasts with nonsense mutations in *CEP290* with mild retinal phenotypes (14). These observations are reminiscent of the Duchenne/Becker muscular dystrophy paradigm (15), which responds to targeted exon skipping therapies (16, 17). Given that most of the CEP290 protein consists of repeated coiled-coil domains, often encoded by a single exon, *CEP290* seems an ideal candidate for ASO-mediated exon skipping therapy.

Results

Clinical and Genetic Investigations. Here we describe a 14 y old boy (JBTS-AA) from consanguineous parents (Fig. 1*A*) affected with JBTS. He initially presented with congenital ptosis and visual

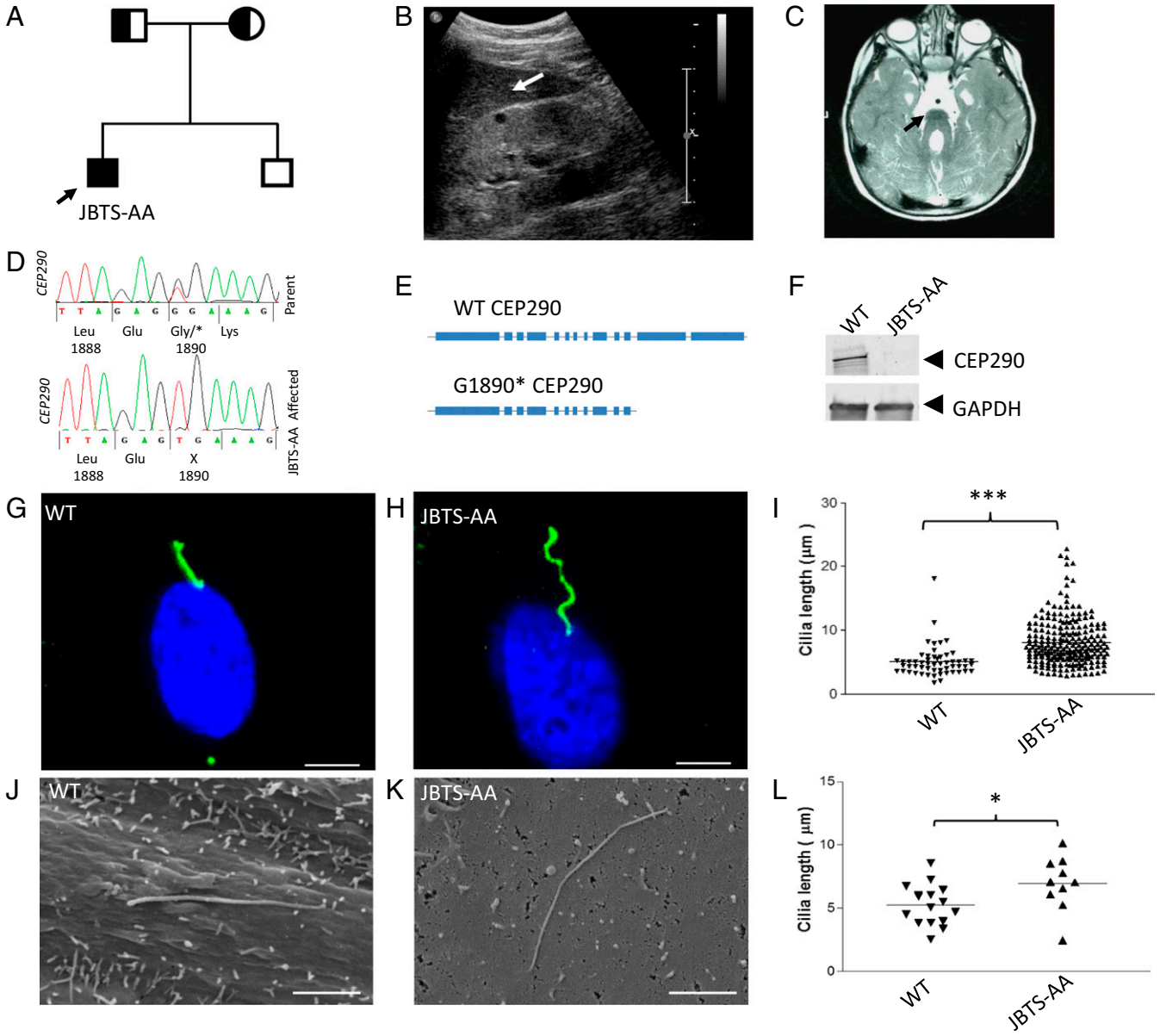

Fig. 1. Clinical phenotype, molecular genetics, and primary cilia defects in human urine-derived renal epithelial cells from a Joubert syndrome patient. (*A*) Pedigree diagram showing single affected male, JBTS-AA (squares, males; circles, females). (*B*) Renal ultrasound scan of JBTS-AA showing minor cystic change within the kidney (arrowed) and loss of corticomedullary differentiation consistent with a diagnosis of nephronophthisis. (*C*) MRI scan of JBTS-AA showing a molar tooth sign (arrowed) with cerebellar vermis aplasia and elongated superior cerebellar peduncles. (*D*) Sequence chromatograms showing homozygous change in *CEP290* c.5668G > T; p.G1890* segregating from parental DNA (father's chromatogram is shown). (*E*) SMART Domain structure of WT CEP290 protein (2,479 amino acids) predicts multiple coiled-coil domains (show as blue bars). The truncated protein CEP290 G1890* results in loss of C-terminal coiled-coil domains. (*F*) Western blotting of protein from human urine-derived renal epithelial cells showing loss of full-length CEP290 protein in JBTS-AA. Blots were probed with a CEP290 antibody directed at the C terminus of CEP290, with GAPDH shown as a loading control. (*G*) Wild-type (WT) and (*H*) patient (JBTS-AA) hURECs imaged under high-power immunofluorescence using anti-ARL13B (green) to identify ciliary membrane. (Scale bar: 5 μm.) (*I*) Quantification of ciliary length in cells grown in serum-free medium for 48 h, measured by immunofluorescence imaging (WT, $n = 55$, JBTS-AA, $n = 222$; ***$P < 0.0001$, unpaired *t* test). (*J*) Wild-type (WT) and (*K*) patient (JBTS-AA) hURECs seen under scanning EM reveals abnormally long cilia in patient cells after 48 h serum starvation (Scale bar: 2 μm.). (*L*) Quantification of increase in cilia length (WT, $n = 16$, JBTS-AA, n = 10; *$P < 0.05$, unpaired *t* test).

failure secondary to an early onset retinal degeneration (*SI Appendix*, Fig. S1) and subsequently developed ataxia and significant renal impairment (Table 1). Clinical investigations revealed hyperechogenic kidneys showing cystic change and loss of corticomedullary differentiation (Fig. 1*B*), consistent with a diagnosis of nephronophthisis, and a "molar tooth" sign on brain MRI (Fig. 1*C*) which is due to cerebellar vermis aplasia and is the defining feature of JBTS. Molecular genetic investigations in JBTS-AA confirmed a homozygous nucleotide substitution leading to a stop codon (c.5668G > T; p.G1890*) in exon 41 of *CEP290* (Fig. 1*D*). This mutation is predicted to lead to a truncated CEP290 protein lacking numerous C-terminal coiled-coil domains (Fig. 1*E*).

Phenotyping Using Primary Renal Epithelial Cells. To characterize the cellular and molecular consequences of this mutation, we derived primary, nontransformed human urine-derived renal epithelial cells (hURECs) from patient JBTS-AA and age/sex matched controls (WT). Western blotting, using a CEP290 C-terminal antibody, confirmed an almost complete absence of full-length CEP290 protein (Fig. 1*F*) from patient hURECs. Immunofluorescence analysis of cilia structure revealed elongated primary cilia on patient hURECs (JBTS-AA) compared with control (WT) cells (Fig. 1 *G–I*). This was confirmed by scanning electron microscopy (Fig. 1 *J–L*). In terms of percentage ciliation rates in hURECs, there was no difference between wild-type and JBTS-AA cells (*SI Appendix*, Fig. S2). We have previously described an elongated cilia phenotype in hURECs derived from an unrelated JBTS patient harboring *CEP290* mutations (9), suggesting abnormally long primary cilia may be a common, renal feature of JBTS. To investigate this further, we carried out immunofluorescence analysis of cilia structure in two further (unrelated) JBTS patients with *CEP290* mutations and kidney failure (*SI Appendix*, Table S1). Immunofluorescence staining of renal biopsies for acetylated tubulin and ARL13B revealed the presence of elongated and tortuous primary cilia in both patients compared with normal kidney (*SI Appendix*, Fig. S3) confirming that the elongated primary cilia found on patient hURECs accurately reflect the phenotype observed in vivo. It is intriguing to note that elongated cilia have also been found in a wide range of other ciliopathy models including: *Bbs-4* null mice (18), *jck* mice (19), Meckel syndrome (20), *Kif7* mutated cells (21), and JBTS secondary to *KIAA0556* mutations (22), suggesting elongated primary cilia may be a widespread feature of ciliopathies in general and that correction of this phenotype attenuates cystic kidney disease (23).

Targeted Exon Skipping of CE290 Rescues Phenotype in Primary Renal Epithelial Cells. Exon 41 of *CEP290* is 123 nucleotides in length and encodes a single, discrete, coiled-coil domain of the protein (*SI Appendix*, Fig. S4). Consequently, a splice-blocking ASO targeted to the splice donor site of exon 41 would be predicted to induce skipping of exon 41, while maintaining the correct reading frame, to produce a transcript encoding a near full-length protein of 2,438 amino acids (286 KDa) that contains a normal C terminus and is lacking only a single coiled-coil domain (*SI Appendix*, Fig. S4). To test the functionality of the splice blocking ASO, we carried out RT-PCR analysis of the *CEP290* transcript from hURECs and confirmed efficient ASO-induced alternative splicing, skipping exon 41 (Fig. 2*A*). In the absence of any available N-terminal CEP290 antibodies, quantitative RT-PCR of the *CEP290* transcript targeted to exons 6–7, upstream of the mutation in JBTS-AA, showed that *CEP290* expression levels in JBTS-AA hURECs are reduced to ∼20% of wild-type levels, suggesting degradation of the mutant mRNA transcript; levels of the transcript are rescued following ASO-induced splicing (*SI Appendix*, Fig. S5*A*). Furthermore, we observed restoration of protein expression by Western blot in ASO-treated JBTS-AA hURECs, with near wild-type levels of protein detectable with the C-terminal CEP290 antibody at 24 h post treatment, which persisted for 96 h (Fig. 2*B*). In addition to the structural ciliary changes observed, JBTS-AA hURECS showed an increase in *SHH* levels (∼fourfold) indicating dysregulation of ciliary signaling. Transcript levels of *SHH* were, however, not fully rescued by ASO treatment (*SI Appendix*, Fig. S5*B*).

Despite lacking a single coiled-coil domain encoded by exon 41, the near full-length CEP290 protein correctly localized to the transition zone in ASO-treated JBTS-AA hURECs (*SI Appendix*, Fig. S6); this provides evidence that the removal of exon 41 in *CEP290* does not affect protein localization. Given the correct localization of the restored protein, lacking a single coiled-coil domain, we investigated whether this could ameliorate the phenotype of JBTS-AA hURECs. Primary cilia were analyzed using fluorescence microscopy directed at ARL13B and a significant reduction in the length of JBTS-AA primary cilia, equivalent to wild-type cilia was observed after 48 h (Fig. 2 *C* and *D*); this was also confirmed by scanning electron microscopy (Fig. 2 *E* and *F*). It is noteworthy that the reduction in cilia length is dramatic and significant even at 24 h, indicating a rapid response to ASO treatment. This extends our previous findings, that pharmacological treatments can reduce cilia length in JBTS hURECs (9), and provides evidence to suggest that this phenotype, which relies upon the continued presence of the mutation, is reversible. Importantly, ASO treatment of wild-type control hURECs had no effect on the length of the primary cilium, suggesting that the absence of the coiled-coil domain encoded by exon 41 can be tolerated.

Targeted Exon Skipping of *Cep290* in Vivo Rescues Ciliary and Cystic Kidney Disease Phenotypes. Having shown a positive effect of ASO treatment on primary, nontransformed patient kidney cells ex vivo,

Table 1. Molecular and clinical characteristics of affected patient (JBTS-AA)

Characteristics	JBTS-AA
Ethnicity and consanguinity	Pakistani, parents first cousins, segregation confirmed
Renal ultrasound scan findings	Increased echogenicity, corticomedullary cysts, loss of corticomedullary differentiation
Kidney function	Chronic kidney disease stage 3, creatinine 1.91 mg/dL (aged 14 y)
Ocular symptoms (age of onset, y)	Congenital ptosis (1 mo) Early onset retinal degeneration initially diagnosed with visual failure (2 mo)
Central nervous symptoms	Ataxia, cerebellar vermis aplasia/hypoplasia with "molar tooth sign" on brain MRI
Nucleotide alterations	Homozygous c.5668G > T (exon 41)
Alteration in coding sequence	Homozygous Gly1890*
Reference sequence	NM_025114
SNP ID	rs137852832
ExAC allele frequency	0.0001432

*Stop codon

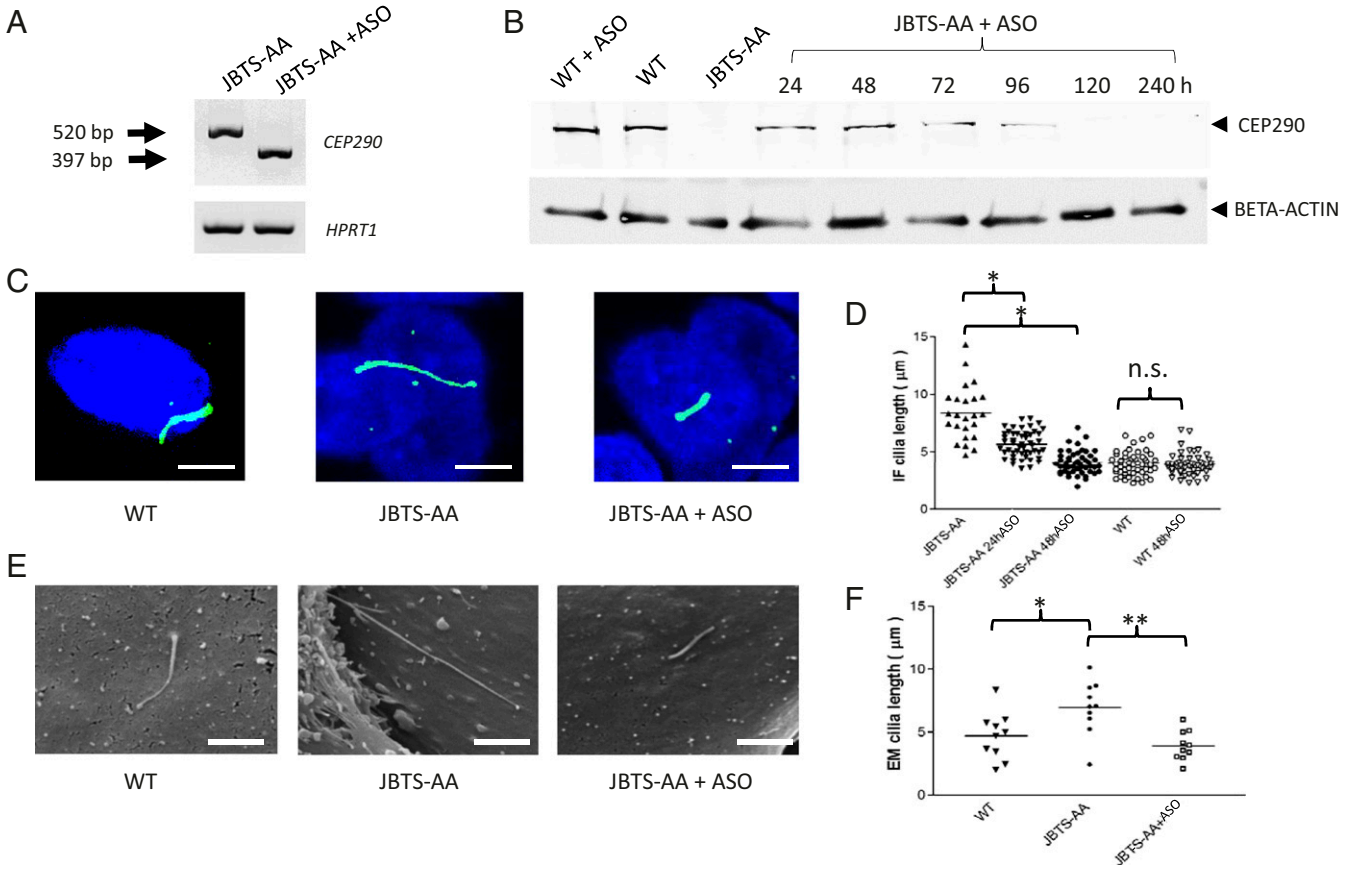

Fig. 2. ASO-induced exon skipping restores CEP290 protein expression and rescues cilia defects in patient hURECs. (*A*) Gene expression analysis using RT-PCR of hURECs obtained from patient JBTS-AA. Lane 1 demonstrates *CEP290* (predicted 520 bp) expression in untreated cells. Lane 2 shows RT-PCR products obtained after treatment with 1 μm ASO directed toward exon 41 splice-junction. ASO-mediated exon skipping leads to a shorter *CEP290* mRNA transcript (predicted product size of 397 bp). (*B*) *CEP290* exon 41 skipping induced by ASO of JBTS-AA hURECs demonstrates the rescue of CEP290 protein translation. WT hURECs protein lysates demonstrate the presence of full-length CEP290 protein (290 kDa), which was not adversely affected by ASO treatment. JBTS-AA hURECs protein lysates show a near absence of full-length protein. JBTS-AA ASO-treated hURECs show rescue of near full-length CEP290 protein translation at 24 h post treatment, which persists for 96 h. BETA-ACTIN (42 kDa) serves as loading control. (*C*) Immunofluorescence (IF) microscopy of wild-type hURECs, untreated JBTS-AA hURECs, and JBTS-AA hURECs treated with ASO to induce exon skipping of exon 41 rescues the phenotype of long cilia. DAPI- blue (Nuclei), Green - ARL13B (Ciliary membrane). (Scale bar: 5 μm.) (*D*) IF quantification of the cilia length in JBTS-AA hURECs followed by treatment with ASO. Cilia length was quantified after treatment with 1 μM ASO at 24 h and 48 h. The mean cilia length measured for untreated JBTS-AA cilia ($n = 24$) was 8.36 μm (detected using ARL13B antibodies). The mean cilia length after treatment with 1 μM ASO for 24 h ($n = 50$) was 4.56 μm and after treatment for 48 h ($n = 50$) was 4.02 μm. The mean cilia length of WT hURECs cilia ($n = 49$) before treatment was 3.96 μm and after treatment with 1 μM ASO for 48 h ($n = 50$) was 3.87 μm. Data are shown as scattergrams with mean shown. *$P < 0.0001$ determined by one-way ANOVA. (*E*) Scanning electron microscopy of hURECs cilia in WT, untreated JBTS-AA, and JBTS-AA treated with ASO and imaged at 48 h. (Scale bar: 2 μm.) (*F*) Electron microscopy (EM) quantification of the cilia length in WT, JBTS-AA, and JBS-AA+ ASO treated hURECs rescued by treatment with ASO. The mean cilia lengths were: WT hURECs 4.8 μm, JBTS-AA 6.74 μm, and JBTS-AA + ASO 3.78 μm. Data are shown as scattergrams with mean indicated.*$P < 0.05$ and **$P < 0.01$, one-way ANOVA. n = 10 cilia for each group. n.s., not significant.

we wished to determine whether a similar strategy could be applied in vivo. The most faithful model of JBTS described to date is the *Cep290*$^{Gt(CC0582)Wtsi}$ mouse line (which we will refer to as *Cep290*^{Gt}, previously reported as *Cep290*^{LacZ}) that presents with a renal-retinal-brain phenotype caused by insertion of a "gene trap" within *Cep290* after exon 25 (8). As the *Cep290*^{Gt} mice were produced from embryonic stem (ES) cells containing an intronic splice acceptor/β-galactosidase/neomycin phosphotransferase (SA-IRES-βGEO) "gene trap" cassette (3,975 bp), we designed a new oligonucleotide to block the splice acceptor of the gene trap cassette (vivo-ASO^{Gt}) to restore full-length Cep290 transcript and protein (*SI Appendix*, Fig. S7). As proof of concept, treatment of immortalized kidney cells derived from homozygous *Cep290*$^{Gt/Gt}$ mice with vivo-ASO^{Gt} resulted in a modest restoration of correct splicing between exons 25 and 26, with a concomitant decrease in exon 25 splicing into SA-IRES-βGEO, and a return of a full-length Cep290 protein detected by Western blotting using a C-terminal Cep290 antibody (*SI Appendix*, Fig. S7). In contrast to ASO treatment of JBTS-AA hURECs, wild-type levels of transcript/protein were not achieved in the transformed mouse cell line following vivo-ASO^{Gt} treatment. RT-PCR analysis with a panel of primers located across the SA-IRES-βGEO cassette suggests that we do not see complete restoration of wild-type transcript levels (*SI Appendix*, Fig. S7), possibly due to the presence of cryptic splice sites within the SA-IRES-βGEO cassette (24, 25). However, given that *CEP290* is not haploinsufficient and it has been reported that small fragments of CEP290 can ameliorate LCA (26), we reasoned that even subwild-type levels of protein may be beneficial. Therefore, we proceeded to investigate the potential effects of a modest restoration of full-length protein in vivo, in *Cep290*$^{Gt/Gt}$ mice. Systemic administration of vivo-ASO^{Gt} was carried out via a series of i.v. injections over 10 d. RT-PCR analysis and sequencing of whole kidney RNA revealed correctly spliced transcripts (Fig. 3*A* and *SI Appendix*, Fig. S8), consistent with splicing from exon 25 to exon 26, skipping SA-IRES-βGEO. Full-length Cep290 protein was detected by a Western blot of whole kidney extracts using C-terminal Cep290 antibody (Fig. 3*B*) indicating that vivo-ASO^{Gt} was capable

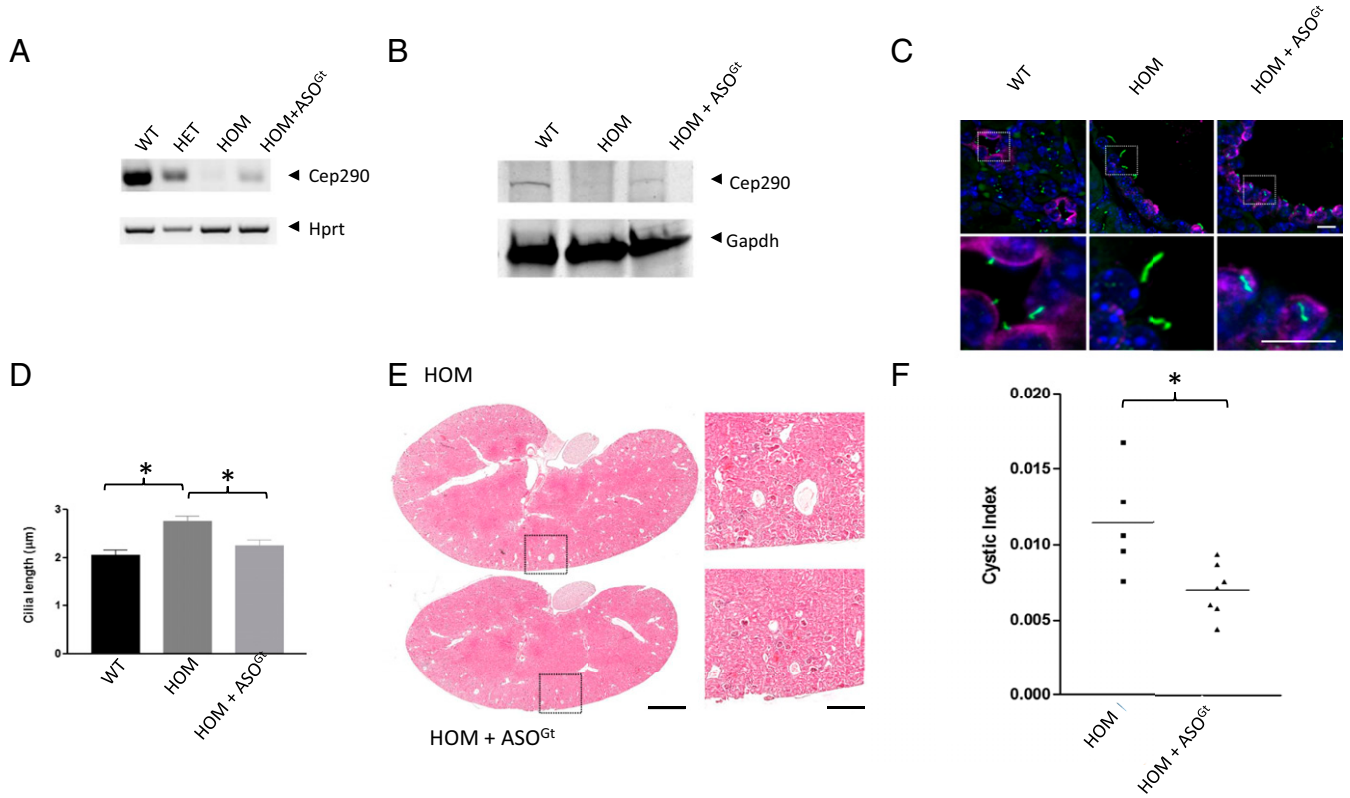

Fig. 3. In vivo systemic ASO treatment restores Cep290 protein expression and reduces cystic burden in a JBTS mouse model. (*A*) RT-PCR of *Cep290* from murine kidney mRNA. RT-PCR products spanning exons 25–27 are shown from kidneys of wild-type (WT), heterozygous $Cep290^{Gt/+}$ (HET), and homozygous $Cep290^{Gt/Gt}$ (HOM) mice. Almost no product is observed when the gene trap is present homozygously. Treatment with *vivo-ASO*^{Gt} of HOM mice increases the amount of wild-type *Cep290* transcript. *Hprt* is shown as a control. (*B*) Western blot showing Cep290 protein isolated from WT, HOM, and HOM mice treated with vivo-ASO^{Gt} to induce skipping of the gene trap. The level of protein in homozygous animals increases in the presence of the ASO^{Gt} treatment. GAPDH (37 kDa) is shown as loading control. (*C*) Immunofluorescence imaging of renal primary cilia within cortical collecting ducts in WT, HOM, and HOM mice treated with vivo-ASO^{Gt}. Cilia are stained with Arl13b (green), collecting ducts are identified using aquaporin-2 (magenta), and nuclei are stained with DAPI (blue). Images are taken from samples with median values of their respective groups. (Scale bar: 10 μm.) (*D*) Quantification of mean primary cilia length from renal tissues of WT ($n = 3$), HOM ($n = 4$), and HOM + ASO^{Gt} treated mice ($n = 7$). Mean number of cilia measured in each animal = 97. (*$P <$ 0.05, one-way ANOVA). (*E*) Hematoxylin and eosin staining of untreated HOM and vivo-ASO^{Gt} treated HOM mice. Images are taken from samples with median values of their respective groups. (Scale bar: 1 mm.) (*F*) Quantification of the cystic index of untreated HOM ($n = 5$) and vivo-ASO^{Gt} treated HOM mice ($n = 7$) at 42 d of age. The mean cystic index is reduced from 0.011 in untreated animals to 0.0069 in animals treated with vivo-ASO^{Gt} (*$P < 0.05$, unpaired *t* test).

of inducing skipping of SA-IRES-βGEO in kidney, in vivo. Whole murine kidney tissue protein extract was used to assess the response of ciliary signaling molecules. Compared with wild-type controls, $Cep290^{Gt/Gt}$ kidneys had increased Shh signaling, as demonstrated by a rise in the Gli3 activator to repressor ratio that was partially restored by treatment with vivo-ASO^{Gt} (*SI Appendix*, Fig. S5 *C* and *D*). Immunofluorescence analysis revealed an increase in the length of primary cilia (Arl13b staining) in cortical collecting ducts (aquaporin-2 staining) in homozygous $Cep290^{Gt/Gt}$ mice compared with wild-type littermates (Fig. 3 *C* and *D*), highlighting a further similarity between the $Cep290^{Gt}$ mouse model and JBTS patients with *CEP290* mutations (*SI Appendix*, Fig. S2). This increase in cilia length of cortical collecting duct cells could be rescued by ∼50% by systemic vivo-ASO^{Gt} treatment, similar to the 24 h ASO treatment of JBTS-AA hURECs. Having shown full-length protein and a shortening of the abnormally long primary cilia following vivo-ASO^{Gt} treatment, we carried out quantitative assessment of cystic burden in vivo-ASO^{Gt} treated and untreated $Cep290^{Gt/Gt}$ kidneys. Remarkably, vivo-ASO^{Gt} treatment resulted in a striking and significant improvement in cystic index (Fig. 3 *E* and *F*) of 37%, indicating that measurable therapeutic benefit can be achieved in vivo by relatively modest levels of ASO-induced splice blocking.

Discussion

We have shown that in human renal epithelial cells from a patient with JBTS secondary to a nonsense mutation in exon 41 of *CEP290*, ASO-mediated exon skipping can ameliorate the ciliary phenotype and restore localization of a near full-length CEP290 protein to the base of the cilium. We have then validated this approach in vivo, by using a different ASO targeting strategy to promote alternate splicing of a murine gene trap insertion within intron 25 of *Cep290*, thereby rescuing, in part, full-length Cep290 transcript and protein to achieve a phenotypic rescue of renal ciliary length in vivo as well as the cystic kidney disease. The observed phenotypic changes in murine and human cells, as well as in mouse kidney tissue following treatment with two completely different ASOs indicate that the observed effects are specific, and result from the restoration of CEP290/Cep290.

Overall, these data have several important implications. Firstly, systemic delivery of ASOs can ameliorate kidney pathology in a whole animal model. In addition, ASOs can rescue disease phenotypes after disease has become established in both JBTS patient-derived cells and an animal model, confirming the indications from pharmacological treatments that the cystic kidney disease is reversible. Finally, ASO-mediated exon skipping is tolerated at the level of protein localization, as the removal of a coiled-coil

domain does not result in the mislocalization of the CEP290 protein. Given that many *CEP290* mutations cluster in the C-terminal coiled-coil-rich region and are potentially skippable (*SI Appendix*, Fig. S9), it is tempting to speculate that these mutations may also be amenable to ASO-mediated therapy.

One limitation of this study is that despite G1890* being one of the most common mutations, we have not extended our human studies to other skippable exons in *CEP290*. Here true personalized medicine approaches, using patient-derived cells, such as we have used with patient JBTS-AA, will be required to determine if exon skipping of alternate exons, which may contain more crucial functional domains than exon 41, are possible. The direct consequences of skipping exons within the *CEP290* gene require testing in both ex vivo and in vivo systems. A *Cep290* mouse model, mimicking the human G1890* mutation, would be required to determine fully the effects of ASO-mediated exon skipping in both kidney and extrarenal tissues. Given the ease of access for subretinal injections, to date there has been a focus on ASO-based therapies for human retinal disease, including *CEP290*-associated LCA (10, 27). As our work has shown, systemic delivery of ASOs is possible and seems to ameliorate kidney disease; this needs to be assessed more fully in renal tissues as well as retinal tissues for dosing regimens and timing of therapies. However, given the efficiency of ASO-mediated exon skipping observed in patient kidney cells, where the next available splice acceptor is used almost exclusively, this is likely to confirm that ASO treatments should be considered as a promising therapeutic approach. It seems likely, following on from the success of ASO-based therapy for targeting *CEP290* retinal disease, that ASO-based therapy for *CEP290*-associated renal disease has true translational promise and may provide a genetic rescuing therapy for this severe ciliopathy syndrome.

In conclusion, we show that using ASO-mediated exon skipping rescues a ciliary defect in patient renal epithelial cells and can be used systemically to target *CEP290* transcripts within kidney tissues, offering a therapeutic approach to treating inherited renal ciliopathies.

Materials and Methods

Study Approval. Ethical approval was obtained from the National Research Ethics Service Committee North East (14/NE/1076), United Kingdom. All animal experiments were conducted according to protocols approved by the Animal Ethics Committee of Newcastle University and the Home Office, United Kingdom.

Statistics. All data are shown as the mean ± SEM, unless otherwise stated and unpaired Student's *t* test or one-way ANOVA followed by a Bonferroni corrected post hoc test when comparing two or more groups. A *P* value of less than 0.05 was considered statistically significant.

Clinical and DNA Sequencing. Following informed and written consent, urine and blood samples were obtained from a 14-y-old boy with clinical JBTS with a retinal, renal, and cerebellar phenotype and a healthy gender- and age-matched control. All methods were performed in accordance with the relevant ethical guidelines and regulations.

Sequencing of Joubert syndrome genes was performed by UKGTN using an 18 Gene Panel (Oxford Regional Genetic Laboratory Service). Confirmation of mutations and segregation analysis was performed on other family members, following informed consent, using Sanger sequencing, using exon specific primers.

In Vitro Studies Using Human Kidney and hURECs. Immunostaining of human kidney tissues from patients with *CEP290* mutations was performed. In vitro studies following hUREC isolation (28), culture, and ASO treatments were performed, including immunostaining, Western blotting, and reverse transcription-PCR and quantitative RT-PCR. Electron microscopy studies were performed on hURECs. Please see *SI Appendix* for detailed materials and methods.

In Vivo ASO Treatment of *Cep290*$^{Gt/Gt}$ Animals. In vivo studies were performed on 28-d-old *Cep290*$^{Gt/Gt}$ animals. Renal tissues were harvested and used for immunofluorescence studies, Western blotting, RNA extraction, and reverse transcription-PCR and quantitative RT-PCR. Please see *SI Appendix* for detailed materials and methods.

ACKNOWLEDGMENTS. Thank you to the patient and family members who contributed to this study. This work is funded by The Medical Research Council (Award MR/M012212/1), a Kidney Research UK Post-doctoral fellowship (to S.A.R.) (Award PDF_003_20151124), and Northern Counties Kidney Research Fund. L.D. is funded by The Medical Research Council Discovery Medicine North Training Partnership.

1. Hildebrandt F, Zhou W (2007) Nephronophthisis-associated ciliopathies. *J Am Soc Nephrol* 18:1855–1871.
2. Valente EM, Brancati F, Boltshauser E, Dallapiccola B (2013) Clinical utility gene card for: Joubert syndrome–update 2013. *Eur J Hum Genet* 21:1187.
3. den Hollander AI, et al. (2006) Mutations in the CEP290 (NPHP6) gene are a frequent cause of Leber congenital amaurosis. *Am J Hum Genet* 79:556–561.
4. Baala L, et al. (2007) Pleiotropic effects of CEP290 (NPHP6) mutations extend to Meckel syndrome. *Am J Hum Genet* 81:170–179.
5. Brancati F, et al.; International JSRD Study Group (2007) CEP290 mutations are frequently identified in the oculo-renal form of Joubert syndrome-related disorders. *Am J Hum Genet* 81:104–113.
6. Leitch CC, et al. (2008) Hypomorphic mutations in syndromic encephalocele genes are associated with Bardet-Biedl syndrome. *Nat Genet* 40:443–448, and correction (2008) 40:927.
7. Betleja E, Cole DG (2010) Ciliary trafficking: CEP290 guards a gated community. *Curr Biol* 20:R928–R931.
8. Hynes AM, et al. (2014) Murine Joubert syndrome reveals Hedgehog signaling defects as a potential therapeutic target for nephronophthisis. *Proc Natl Acad Sci USA* 111: 9893–9898.
9. Srivastava S, et al. (2017) A human patient-derived cellular model of Joubert syndrome reveals ciliary defects which can be rescued with targeted therapies. *Hum Mol Genet* 26:4657–4667.
10. Garanto A, et al. (2016) In vitro and in vivo rescue of aberrant splicing in CEP290-associated LCA by antisense oligonucleotide delivery. *Hum Mol Genet* 25:2552–2563.
11. Littink KW, et al. (2010) A novel nonsense mutation in CEP290 induces exon skipping and leads to a relatively mild retinal phenotype. *Invest Ophthalmol Vis Sci* 51:3646–3652.
12. Burnight ER, et al. (2014) CEP290 gene transfer rescues Leber congenital amaurosis cellular phenotype. *Gene Ther* 21:662–672.
13. Drivas TG, Wojno AP, Tucker BA, Stone EM, Bennett J (2015) Basal exon skipping and genetic pleiotropy: A predictive model of disease pathogenesis. *Sci Transl Med* 7:291ra97.
14. Barny I, et al. (May 16, 2018) Basal exon skipping and nonsense-associated altered splicing allows bypassing complete CEP290 loss-of-function in individuals with unusually mild retinal disease. *Hum Mol Genet*, 10.1093/hmg/ddy179.
15. Klein CJ, et al. (1992) Somatic reversion/suppression in Duchenne muscular dystrophy (DMD): Evidence supporting a frame-restoring mechanism in rare dystrophin-positive fibers. *Am J Hum Genet* 50:950–959.
16. van Deutekom JC, et al. (2007) Local dystrophin restoration with antisense oligonucleotide PRO051. *N Engl J Med* 357:2677–2686.
17. Kinali M, et al. (2009) Local restoration of dystrophin expression with the morpholino oligomer AVI-4658 in Duchenne muscular dystrophy: A single-blind, placebo-controlled, dose-escalation, proof-of-concept study. *Lancet Neurol* 8:918–928.
18. Mokrzan EM, Lewis JS, Mykytyn K (2007) Differences in renal tubule primary cilia length in a mouse model of Bardet-Biedl syndrome. *Nephron Exp Nephrol* 106:e88–e96.
19. Smith LA, et al. (2006) Development of polycystic kidney disease in juvenile cystic kidney mice: Insights into pathogenesis, ciliary abnormalities, and common features with human disease. *J Am Soc Nephrol* 17:2821–2831.
20. Tammachote R, et al. (2009) Ciliary and centrosomal defects associated with mutation and depletion of the Meckel syndrome genes MKS1 and MKS3. *Hum Mol Genet* 18: 3311–3323.
21. He M, et al. (2014) The kinesin-4 protein Kif7 regulates mammalian Hedgehog signalling by organizing the cilium tip compartment. *Nat Cell Biol* 16:663–672.
22. Sanders AA, et al. (2015) KIAA0556 is a novel ciliary basal body component mutated in Joubert syndrome. *Genome Biol* 16:293.
23. Husson H, et al. (2016) Reduction of ciliary length through pharmacologic or genetic inhibition of CDK5 attenuates polycystic kidney disease in a model of nephronophthisis. *Hum Mol Genet* 25:2245–2255.
24. Roshon M, DeGregori JV, Ruley HE (2003) Gene trap mutagenesis of hnRNP A2/B1: A cryptic 3′ splice site in the neomycin resistance gene allows continued expression of the disrupted cellular gene. *BMC Genomics* 4:2.
25. Anson DS, Limberis M (2004) An improved beta-galactosidase reporter gene. *J Biotechnol* 108:17–30.
26. Zhang W, Li L, Su Q, Gao G, Khanna H (2018) Gene therapy using a miniCEP290 fragment delays photoreceptor degeneration in a mouse model of Leber congenital amaurosis. *Hum Gene Ther* 29:42–50.
27. Gerard X, Garanto A, Rozet JM, Collin RW (2016) Antisense oligonucleotide therapy for inherited retinal dystrophies. *Adv Exp Med Biol* 854:517–524.
28. Ajzenberg H, et al. (2015) Non-invasive sources of cells with primary cilia from pediatric and adult patients. *Cilia* 4:8.